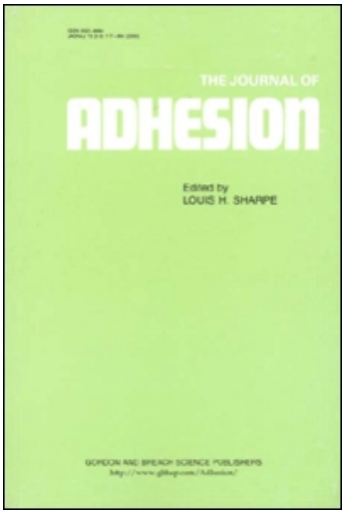

The Journal of Adhesion
Publication details, including instructions for authors and subscription information:
http://www.informaworld.com/smpp/title~content=t713453635

Effect of Pressure Cycling on Fracture Energy of Polyurethane/Aluminum Adhesive Bonds

Alyre Maclure[a]; Vijaya B. Chalivendra[a]; Thomas Ramotowski[b]
[a] Department of Mechanical Engineering, University of Massachusetts, North Dartmouth, MA, USA [b] Devices, Sensors and Materials R&D Branch, Naval Undersea Warfare Center, Newport, RI, USA

Online publication date: 19 November 2009

To cite this Article Maclure, Alyre , Chalivendra, Vijaya B. and Ramotowski, Thomas(2009) 'Effect of Pressure Cycling on Fracture Energy of Polyurethane/Aluminum Adhesive Bonds', The Journal of Adhesion, 85: 12, 869 — 888
To link to this Article: DOI: 10.1080/00218460903307746
URL: http://dx.doi.org/10.1080/00218460903307746

The Journal of Adhesion, 85:869–888, 2009

ISSN: 0021-8464 print/1545-5823 online
DOI: 10.1080/00218460903307746

Taylor & Francis
Taylor & Francis Group

Effect of Pressure Cycling on Fracture Energy of Polyurethane/Aluminum Adhesive Bonds

Alyre Maclure[1], Vijaya B. Chalivendra[1], and Thomas Ramotowski[2]
[1]Department of Mechanical Engineering, University of Massachusetts, North Dartmouth, MA, USA
[2]Devices, Sensors and Materials R&D Branch, Naval Undersea Warfare Center, Newport, RI, USA

An experimental study was conducted to investigate the effect of pressure-cycling on adhesive bond fracture energy of polyurethane/aluminum adhesive bond joints. Initially, two types of peel tests were conducted to characterize adhesive bond strength and challenges associated with pre-mature polyurethane cracking and failure during these tests are discussed. A modified double cantilever beam (MDCB) specimen configuration was specially designed and opening-mode loading conditions were employed to determine the interfacial adhesive bond energy (G_C). The test specimens were pressure-cycled in water-filled tanks for 1 to 4 weeks with an increment of 1 week. The G_C of pressure-cycled specimens was compared with both control and water-soaked samples (without pressure-cycling). The results indicated that pressure-cycling decreased G_C values to those of the control and water-soaked samples: hence, prolonged pressure-cycling could be problematic to polymer/metal adhesive bonds of hardware installed outboard of submarine pressure hulls.

Keywords: Aluminum 6061; Interfacial adhesive fracture energy; Modified double cantilever specimen; Peel testing; Polyurethane; Pressure-cycling; Primer

1. INTRODUCTION

Fracture near the interface of two dissimilar materials is quite common in many industrial, aerospace, and navy applications. Specifically, fracture near the interface has been investigated in several

Received 17 December 2008; in final form 2 June 2009.
Address correspondence to Vijaya B. Chalivendra, Department of Mechanical Engineering, University of Massachusetts, Group-II, 116, 285 Old Westport Road, North Dartmouth, MA 02747, USA. E-mail: vchalivendra@umassd.edu

applications of medical replacements, functionally graded materials, the coating industry, the electronics industry, and in various pressure vessel applications including large gas containers and nuclear pressure vessels [1–5]. In the above applications, polymer/metal adhesive bonds and their interfacial failure is of paramount importance. There were various studies reported on interfacial fracture of polymer/metal adhesive systems in the literature. Venables [6] presented various factors responsible for promoting the integrity and long-term durability of metal-polymer bonds used in the fabrication of aircraft and aerospace structures in his review article. Nitsché [7] conducted a micro-analytical study on the metal/polymer interface in aluminum adhesive joints. In their study, they identified mechanical anchoring of the adhesive within the oxide pores of the metal substrate as the predominant adhesion mechanism. Dauskardt *et al.* [8] studied adhesion and progressive delamination of polymer/metal interfaces under cyclic fatigue loading and found that interface fracture resistance was strongly dependent on the interface morphology and the thickness of the polymer layer. Bistac *et al.* [9] reported that the viscoelastic properties of polymers have significant influence on the rate sensitive adhesive behavior of steel/polymer/steel assemblies. Recently, Deb *et al.* [10] conducted experimental and analytical studies on the mechanical behavior of adhesively bonded joints using double lap shear coupon tests for variable extension rates and temperatures. They identified that, at a high temperature, the adhesive joints exhibit a greater degree of strain rate sensitivity with a significant fall in joint strength. However, at a low temperature, joint strength remains comparable with that at room temperature. Very recently, Shatil *et al.* [11] studied ductile-brittle fatigue and fracture behavior of aluminum/PMMA bimaterial three-point bend specimens both experimentally and numerically for mode-I and mixed-mode stress intensity factors. In their study, they reported that bimaterial fatigue crack growth is dominantly elastic with a small plastic zone near the crack-tip. In relation to the effect of environmental conditions on metal/polymer adhesive bond strength, very little work has been reported. Venables [6] discussed, in his review article, the environmental stability of the morphology of the surface oxide of metal on the integrity of metal/polymer bonds and also proposed that the durability of adhesive bonds to aluminum can be achieved using a treatment in which monolayer films of certain organic acids are applied to the adherend oxide to protect it against the effects of moisture. Toivola *et al.* [12] conducted four-point delamination tests to measure the effect of environmental exposure on the fracture characteristics of polymethylmethacrylate (PMMA)-titanium and PMMA-aluminum interfaces. The degradation

of the interfaces of the above two systems on water exposure was connected to a hydrolysis reaction reversing the original bonding between the PMMA and the hydrolyzed native metal oxides.

In all the above studies, the specimens were tested without exposing them to any a hydrostatic pressure-cycling. However, in navy applications, hardware installed outboard of submarine pressure hulls may have multiple polymer/metal adhesive bonds that are frequently subjected to cyclic pressure changes. The effect of recurring hydrostatic pressure-cycles on the adhesive strength of metal/polymer bonds has not been investigated in the literature. It is important for the naval applications to incorporate accurate adhesive strength values that have been obtained from pressure-cycled samples into hardware reliability models for submarines (specifically underwater cable connectors). To prevent unexpected/unanticipated in-service failures, in this paperpolyurethane/aluminum adhesive bond joints were tested using a modified double cantilever specimen configuration. The effect of pressure-cycling (1 to 4 weeks in increments of 1 week) on the interfacial fracture energy of these adhesive joints was investigated and the results are compared with both dry control specimens and water-soaked samples not subjected to pressure-cycling.

The outline of the article is as follows. In Section 2, the experimental details of peel testing and some challenges associated with peel testing are discussed. In Section 3, the details of the modified double cantilever beam specimen configuration and the experimental scheme of pressure-cycling, water-soaking, and control specimens are discussed. In Section 4, the results of experiments and statistical analysis of the experimental data are provided. Section 5 presents the conclusions of the study.

2. EXPERIMENTAL CHALLENEGES OF PEEL TESTING

2.1. 90° Peel Tests Specimen Configuration

Figure 1 shows a schematic of the 90° peel test specimen configuration as proposed in ASTM Standard D6862-04 [13]. The metal/polymer adhesive bond system consisted of aluminum 6061-T6 (General Supplies, New Bedford, MA, USA), polyurethane FH3140 (H.B. Fuller, St. Paul, MN, USA), and industrial primer (PR-420, PRC-Desoto International, Inc., Glendale, CA, USA) that was used to bond these two materials to each other. A 1.6-mm thick × 25.4-mm wide × 150-mm long aluminum strip was used as the metal substrate. First, the aluminum substrate was sandblasted with 60 grit aluminum oxide media at 414 kPa pressure. The metal substrate was then immediately

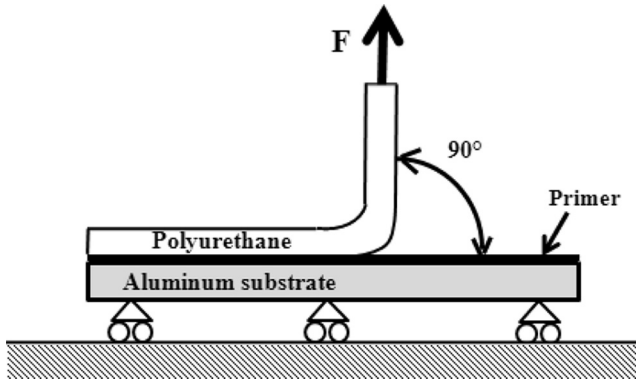

FIGURE 1 A schematic of 90° peel testing specimen configuration.

solvent-cleaned with acetone and primed. Since the primer viscosity was about the same as water, the thickness of the deposited primer layer was only 20 micro meters as measured by a micrometer. The primer was open air cured for 1 hour before being placed in a fixture for molding. The polyurethane used in this study consisted of two parts: resin (part-A) and hardener (part-B). The mix ratio of these two parts was 100(resin):22(hardener) by weight. For a given amount of mix, the proportional amounts were hand mixed and degassed under vacuum to remove any air bubbles generated during the hand mixing process. A pre-crack was made using Teflon® tape that prevents the bonding of the primer to the aluminum surface. The polyurethane mix was then poured into the specimen mold and allowed to cure at room temperature for 24 hours. The finished specimen had a polyurethane strip roughly 6.25 mm thick bonded to the aluminum substrate through the primer. Specimen edges were band saw cut and sanded after demolding to remove excess material beyond the edges of the aluminum substrate. Fabricated specimens were treated in groups of both pressure-cycling and water-soaking, and compared with a control (with neither pressure-cycling nor water-soaking). Pressure-cycling was performed in a closed water tank at 70°F (21°C) hours, cycling from 0–6.9 MPa for 2 hours and holding at 4.14 MPa for the remaining 2 hours.

2.2. Experimental Results & Discussion on 90° Peel Tests

Figure 2 shows typical load-displacement diagrams for specimens of all types: control, pressure-cycled, and water-soaked. All three conditions

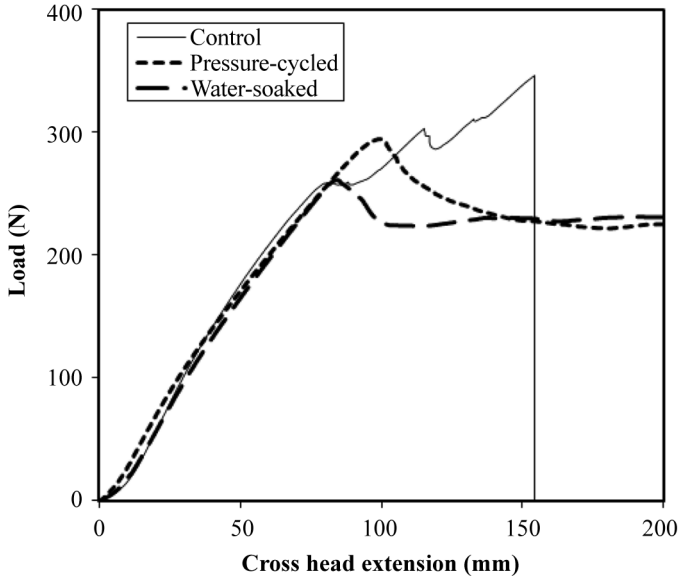

FIGURE 2 Typical load *vs.* displacement diagrams of 90° peel test.

show a similar linear portion and the control specimens showed a maximum peak value compared with the other two. However, both pressure-cycled and water-soaked samples showed increased displacement and the control specimen failed at around 155 mm cross-head displacement because of cracking in the polyurethane and resulting fracture. The reason for the prolonged extension of pressure-cycled and water-soaked samples that the polyurethane absorbs some water which caused it to soften and become plasticized. The major failure mode for the 90° peel tests of all three types of specimens is polyurethane edge cracking and failure as shown in Fig. 3. Most of the strain energy stored in the specimen is spent for premature edge cracking of the polyurethane and only part of it is available for interfacial delamination. Since the energy required to fracture the polyurethane is smaller than that required for delamination, no further adhesive debonding takes place. The polyurethane also elongates significantly while peeling and the energy spent on this deformation needs to be accounted for in the force-displacement diagrams to obtain the adhesive debonding energy. For these reasons, the force-deflection diagrams shown in Fig. 2 are not representative of pure adhesive failure.

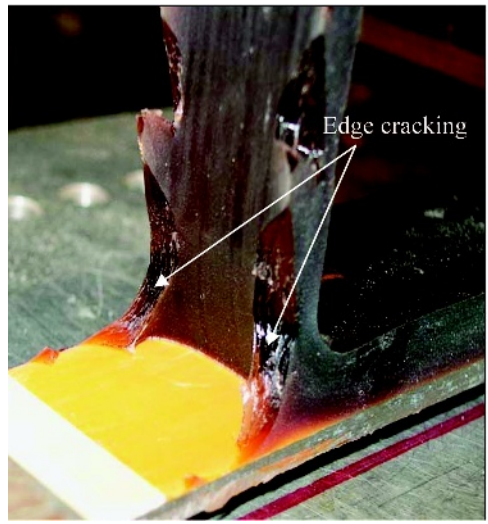

FIGURE 3 Typical cracking and failure of polyurethane during 90° peel tests.

2.3. Circular Peel Test Specimen Configuration

Due to the shortcomings of the 90° peel tests, circular peel tests were investigated. The circular peeling of the polyurethane was performed on cylindrical aluminum substrates. The proposed circular peel tests are closer to realistic peeling situations for undersea cable connectors than are the 90° peel tests. A specimen with a tubular 6061-T6 aluminum substrate of 150-mm diameter along with a polyurethane strip of 25.4-mm width, as shown in Fig. 4, was used to perform circular peel

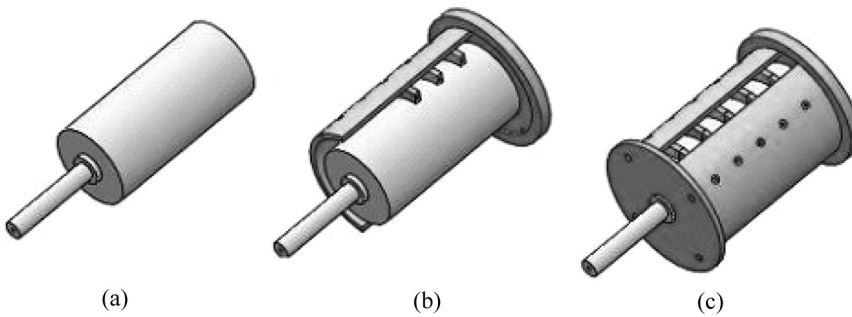

FIGURE 4 Schematic showing molding apparatus used for circular peel: (a) hollow mandrel, (b) sectional view to reveal partitions, and (c) complete assembly.

tests. Such a specimen configuration was inspired by mandrel peeling configurations [14,15]. In an attempt to prevent the polyurethane strips from cracking before adhesive failure occurs, the thickness of the polyurethane strip was increased to 12.5 from 6.25 mm. In order to test several test specimens mounted on a single setup, a special fixture was constructed. Figure 4 shows the molding apparatus used to create the circular peel specimens. A hollow mandrel as shown in Fig. 4(a) is encased with two end caps and five specimen partitions. The partitions define each specimens's width and keep them separate as shown in Fig. 4(b). Finally an exterior shell encompasses the mold as shown in Fig. 4(c). This shell mates to the partitions ensuring the strip thickness is even for 350°. The remaining 10° is left open as a fill area for the mold. The mold produces six specimen strips. The 10° of uncontrolled specimen thickness is discarded. A single strip is shown in Fig. 5. An initial crack was again made with Teflon® tape and the polyurethane strip was pulled as shown in Fig. 5.

2.4. Experimental Results & Discussion on Circular Peel Tests

Typical results of force-displacement plots of the circular peel tests are shown in Fig. 6. Only 1 week of pressure-cycling data was used in comparison with the control sample because the polyurethane failed again *via* cracking without interfacial failure. As can be seen in Fig. 6 the

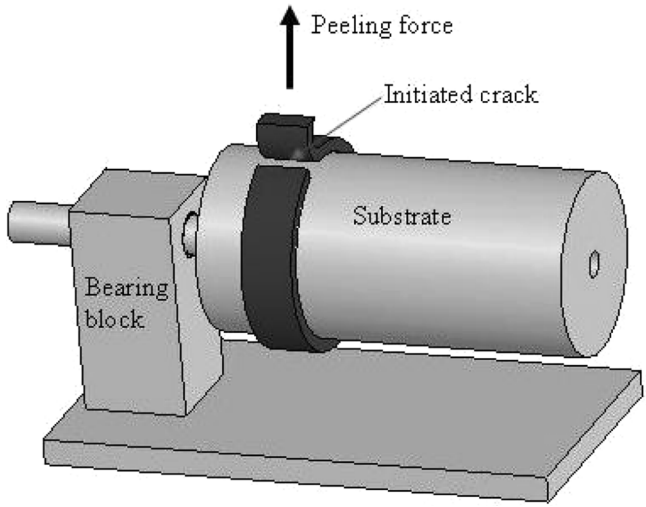

FIGURE 5 The loading configuration used for circular peeling test.

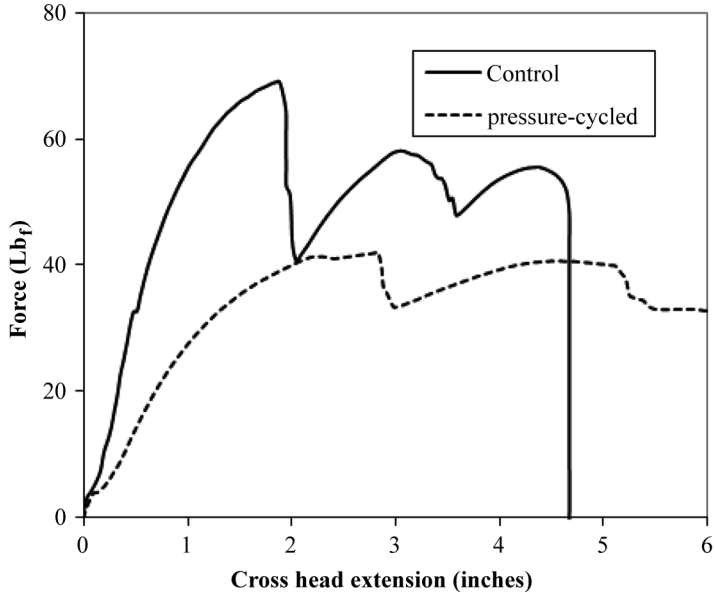

FIGURE 6 Load *vs.* displacement diagram of circular peel tests.

control sample had a sharp drop in load. This drop is due to the same edge thickness cracking as seen in the 90° peel. Also, the load *vs.* displacement diagram for the pressure-cycled circular peel samples is qualitatively similar to that for the 90° peel test samples. The pressure-cycled specimens elongated much more than the control samples. Rather than a sharp load drop, this specimen configuration is able to sustain more interfacial fracture before through thickness cracking predominates. For the above reasons, no water-soaked samples were tested for the circular peel tests.

3. EXPERIMENTAL STUDIES ON MDCB SPECIMEN CONFIGURATION

It can be seen from the above section that edge cracking of the polyurethane is inevitable in both 90° peel and circular peel test specimens. The experimental data in the force-deflection diagrams obtained from the specimens are meaningless unless the large deformation energy and fracture energy of the edge is properly accounted for something that is quite challenging. These challenges led to the design of a special specimen configuration that could provide valid quantitative adhesive bond fracture energies without any edge cracking.

3.1. MCDB Specimen Configuration

A modified double cantilever beam (MDCB) specimen as shown in Fig. 7 was designed to characterize the adhesive bond strength of the polyurethane/aluminum adhesive joint. The specimen consists of a rectangular polyurethane (FH-3140) slab sandwiched between and bonded to two aluminum 6061-T6 substrates of equal width (25.4 mm) using the industrial primer (PR-420). The other dimensions of the specimen are shown in Fig. 7. Since the polyurethane is a soft elastomer, a second aluminum substrate was added on the top of the polyurethane so that polyurethane does not undergo much elongation while separating the bond at the bottom interface where there is an

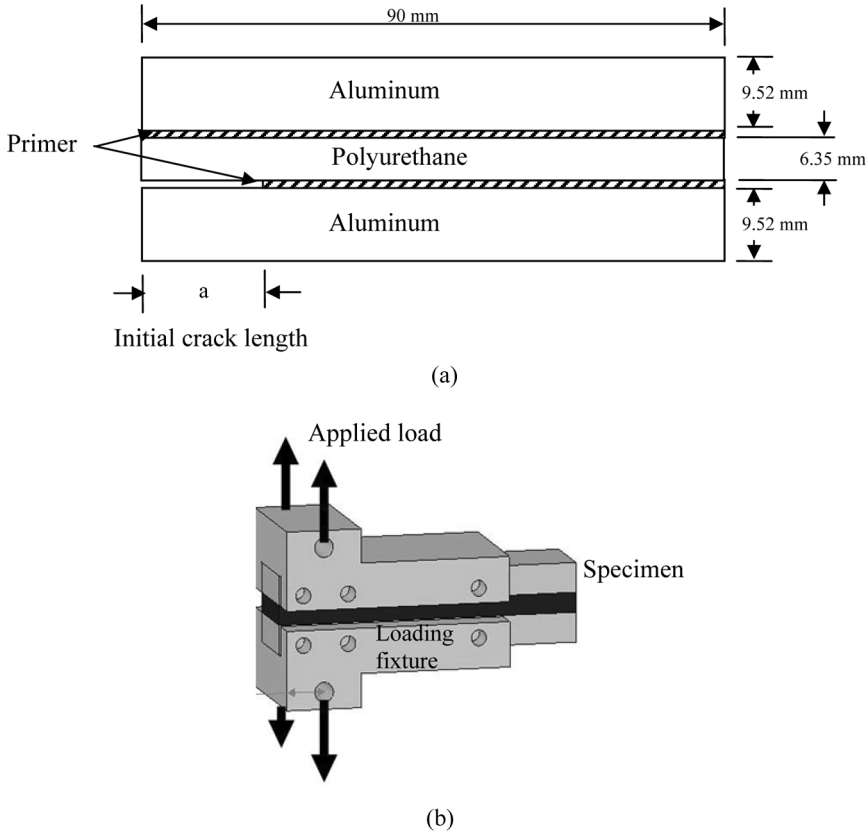

FIGURE 7 (a) Modified double cantilever beam configuration. (b) Loading fixture configuration.

initial crack. A simple procedure was employed to make the specimen. First, the aluminum slabs were degreased with a detergent and later the bonding surfaces were media blasted with 60 grit aluminum oxide at an air pressure of 414 kPa. Second, the aluminum bonding surfaces were solvent-washed with isopropul alcohol. An initial crack was formed by masking the bottom aluminum substrate [shown in Fig. 7(a)] with masking tape. The initial crack lengths were produced with a taping fixture providing ± 0.508 mm accuracy. The unmasked surface of aluminum was painted with PR-420 industrial primer as discussed above. Four different initial crack lengths (25.40, 31.75, 38.10, and 44.45 mm) were used in this study. After applying the primer, the specimens were cured under a vacuum for 1 hour. Curing under vacuum ensured a consistent environment void of excessive water vapor which can bond to the primer's isocyanate groups rendering them inactive for polyurethane bonding [16]. The manufacturer recommends curing the primer for 1–4 hours before polyurethane application. After curing the primer on the aluminum strips, the strips were placed in a fixture and degassed polyurethane mix was poured inside. The mold was left to cure for 96 hours at room temperature before the samples were removed for testing.

A schematic of the loading fixture and the actual loading conditions for a MDCB specimen are shown in Fig. 7(b). As shown in the figure, a thick steel fixture was locked to each aluminum substrate of the MDCB specimen. The fixture provides accuracy and repeatability of crack-tip positioning with respect to the point of loading. The point of loading was 12.7 mm away from the specimen edge or half of the smallest crack length. Load was applied through pin connections allowing a symmetric opening as the load increased.

Pressure-cycling was performed in tap water. The reason for using fresh tap water instead of seawater (which is the true medium of pressure-cycling for most navy vessels) was to reduce the rate of corrosion of the steel vessels used for pressure-cycling. All specimens were placed into the tank at one time and a set of specimens were removed at weekly intervals. The cycles had a maximum pressure of 6,894 kPa and a 30 minute dwell time at zero pressure. The ramp time to reach the maximum from zero was 3 minutes and the maximum pressure was applied for 30 minutes as shown in Fig. 8. Each week of cycling consisted of approximately 150 cycles.

Water-soak specimens were left submerged in tap water in a covered container for the same duration as their pressure-cycled counterparts. Adequate space was left surrounding each specimen to ensure uniform water exposure. Specimens were tested within an hour after removal from the container.

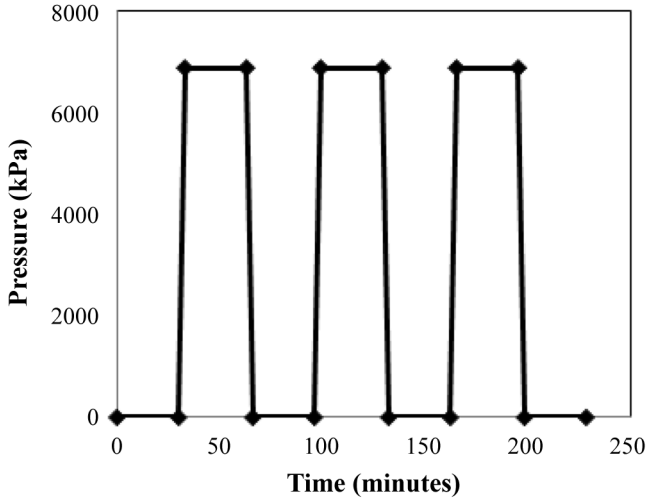

FIGURE 8 Schematic representing pressure-cycling details.

3.2. Design of MCDB Specimen Experiments

Previous experiments reported [17,18] in the literature on the determination of adhesive fracture energy used only one DCB specimen with a known crack length at the start. New cracks were generated in the same specimen with repeated loading and unloading. The load-displacement diagrams for multiple crack lengths on the same specimen were used to determine G_C. There are two limitations on using a single specimen with multiple crack lengths in this study. They are: (a) the new crack generated during the loading process is curved and the crack length measurement is ambiguous, and (b) the new crack front is not exposed to pressure-cycling or water-soaked conditions. Hence, in this study, several specimens of pre-determined initial crack lengths were made and exposed to pressure-cycling or water-soaking. Although more specimens are required, this method alleviates both of the above concerns. The testing scheme consisted of 9 levels: specimen exposure to 1–4 week pressure-cycling, 1–4 week water-soaking and control (no pressure-cycling & no water-soaking). Within one level, four random specimens (25.40, 31.75, 38.10, and 44.45-mm crack lengths) were grouped to produce a specimen representing one master specimen. The calculations for G_C require data at each initial crack length, hence such groupings were essential. Combining specimens in this way gives robustness to the experimental procedure as it

employs randomization to the fullest extent. All specimens were created in groups of approximately (one polyurethane mix batch) and randomly selected for each level.

An Instron 5500 R material testing system (Instron, Norwood, MA, USA) was used to load the specimen and record the load-displacement curves for specimens of different crack lengths. Each specimen was loaded at a rate of 6.35 mm/min and the test was stopped when the load drop was noticed due to initiation of the crack. From the linear portion of the load-displacement diagram, the slope ($\Delta P/\Delta\delta$) was determined and peak critical load (P_{cr}) was also recorded for each specimen. Next, P_{cr} was plotted against initial crack length. Using the slope ($\Delta P/\Delta\delta$), its inverse was calculated, which is also called compliance. Next, compliance *vs.* crack length was plotted and the slope ($\partial C/\partial a$) was obtained as a function of crack length. Representative plots of force *vs.* displacement, peak critical load *vs.* initial crack length, and compliance *vs.* crack length are shown in Figs. 9 through 11, respectively. Interfacial fracture energy was calculated as in Equation 1 [17].

$$G_C = \left(\frac{P_{cr}^2}{2W}\right)\left(\frac{\partial C}{\partial a}\right), \tag{1}$$

where W is the width of the specimen.

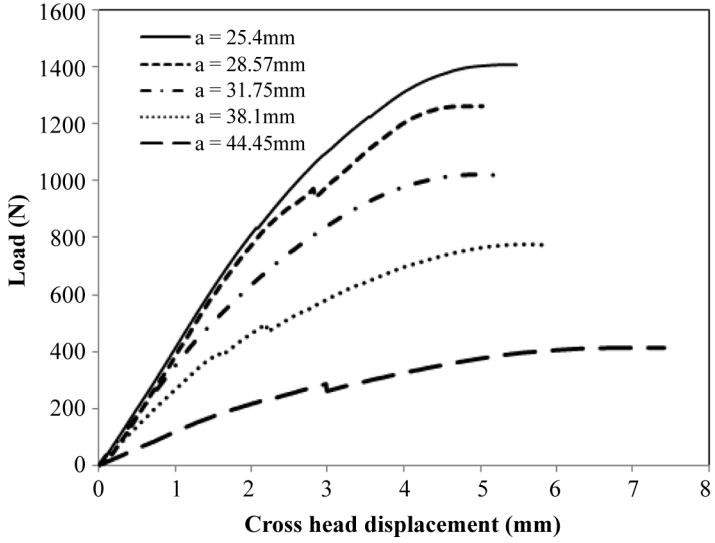

FIGURE 9 Load *vs.* displacement diagrams as a function of crack lengths.

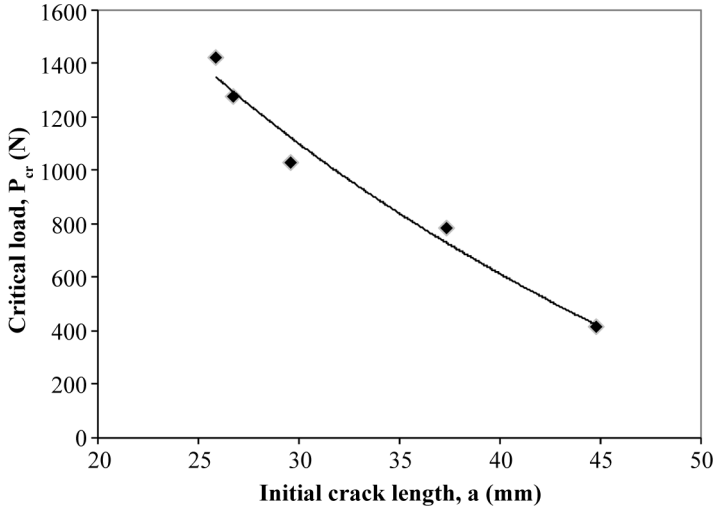

FIGURE 10 Variation of critical load (P_{cr}) as a function of initial crack length (a).

4. RESULTS AND DISCUSSION

Using the above discussed procedure, G_C values were determined as a function of crack length for all three types of specimens. The variation of G_C for control samples (without pressure-cycling & water-soaking)

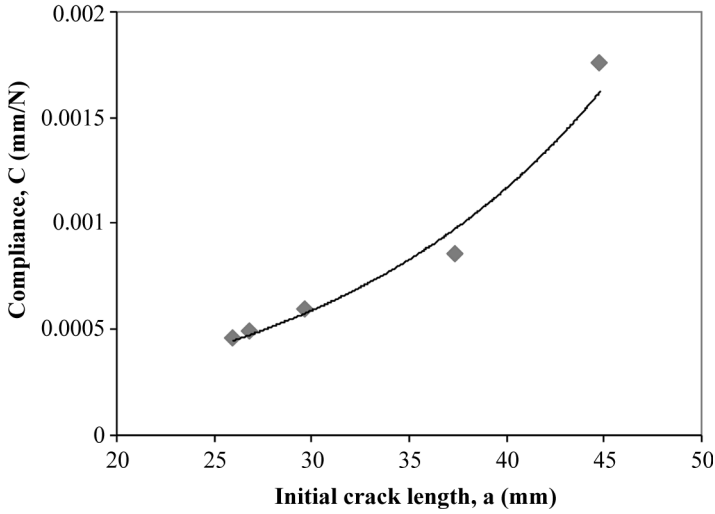

FIGURE 11 Variation of specimen compliance against initial crack length.

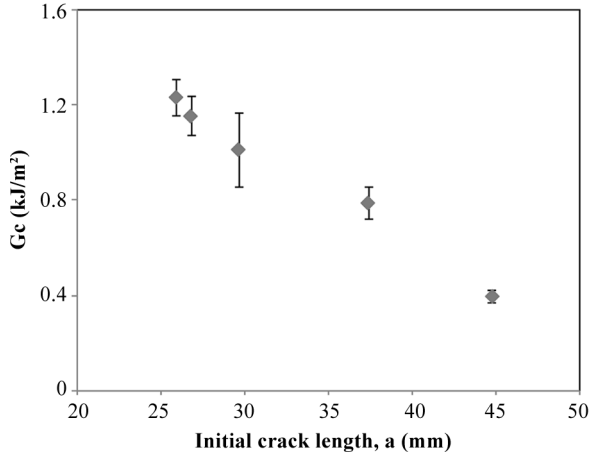

FIGURE 12 Variation of G_C as a function of initial crack length.

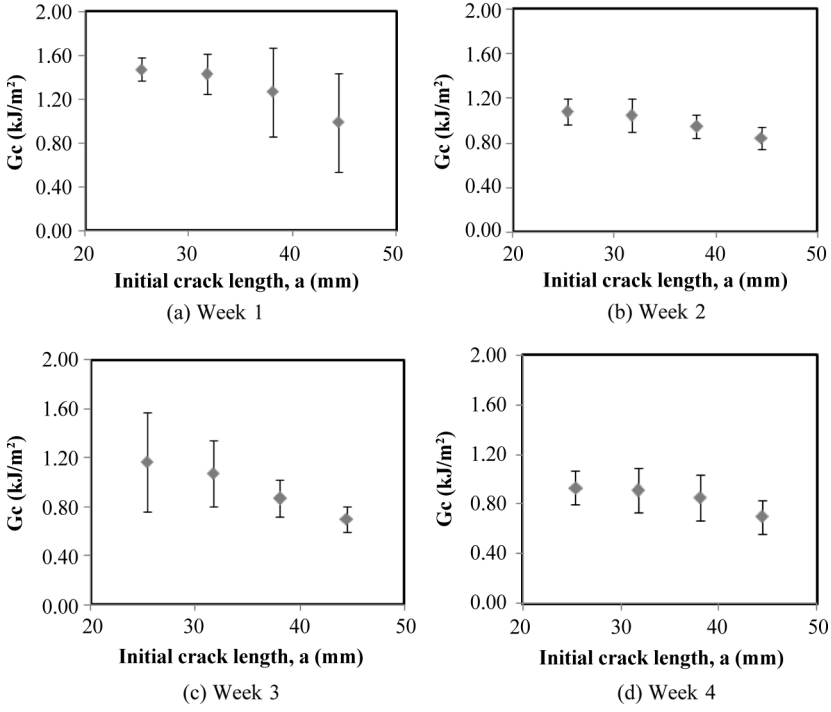

FIGURE 13 Fracture energy values of pressure-cycled specimens for 4 different weeks.

is shown in Fig. 12. The error bars were determined by using Student t-distribution with 95% confidence level. In Fig. 12, the G_C values are relatively constant until a 31.75-mm initial crack length and they decrease at higher crack lengths. This is due to the fact that as the crack length increases, the specimen's end conditions play a more predominant role and the G_C values are no longer valid at those crack lengths. The results of G_C values for four different weeks of pressure-cycled and water-soaked specimens are shown Figs. 13 and 14, respectively. It can be seen from Figs. 13 and 14 that as the crack length increased, the G_C values decreased. This is again attributed to specimen end effects.

Figure 15 shows a comparison of G_C values for both pressure-cycled and water-soaked specimens against control specimens as a function of time. To eliminate specimen end effects, G_C values of only the first three crack lengths from Figs. 12, 13, and 14 are plotted in Fig. 15. The G_C value of the control samples are plotted at zero weeks and the two

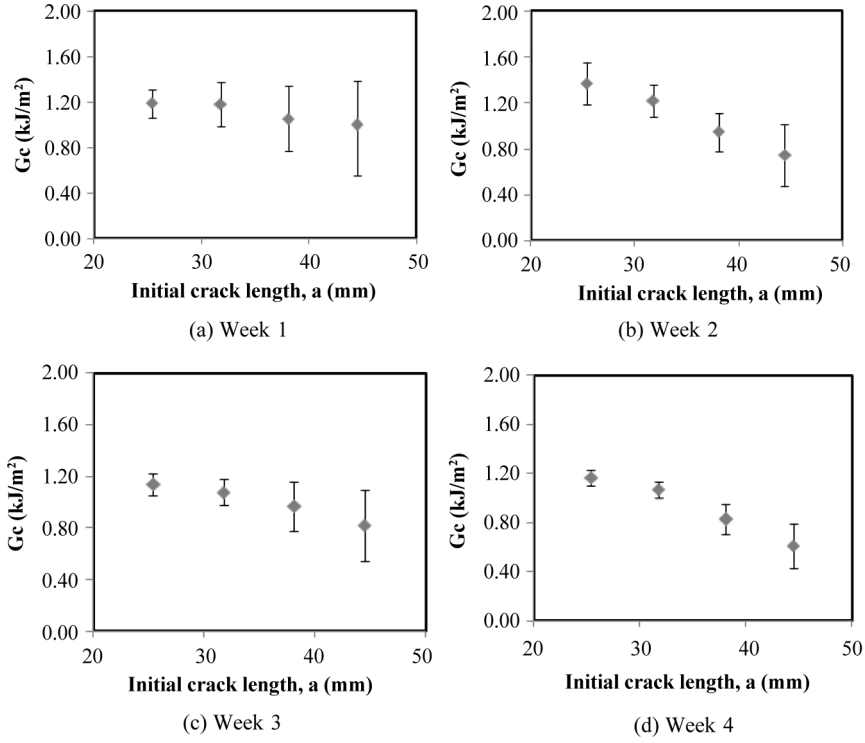

FIGURE 14 Fracture energy values of water-soaked specimens for 4 different weeks.

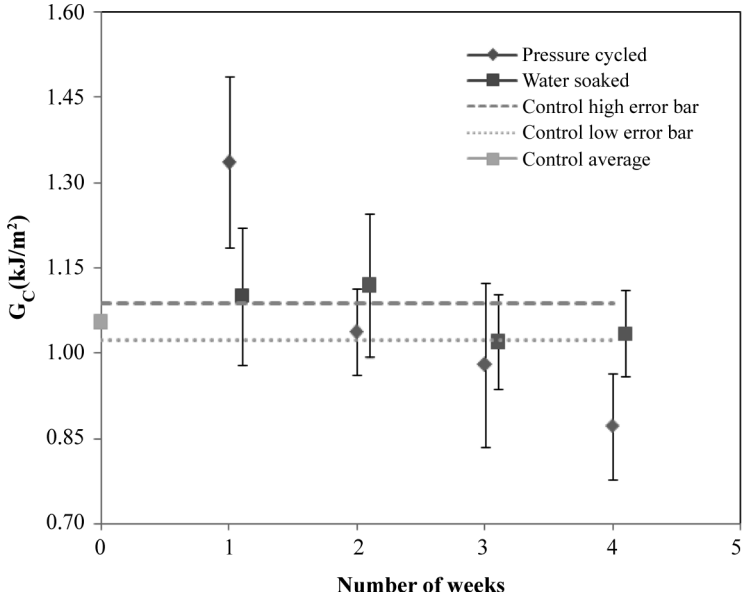

FIGURE 15 Consolidated G_C values of all three types as a function of number of weeks (water-soaked data are intentionally shifted slightly for clarity).

horizontal lines are upper and lower error bar lines for these samples. Figure 15 indicates that pressure-cycling specimens show an overall decreasing trend as the number of weeks increases. There is a surprising increase in the G_C value after 1 week of pressure-cycling compared with the control specimens and the reasons for this are not clear. Even though the water-soaked specimens show no such decrease compared with pressure-cycled specimens, there is a slight decrease in G_C values in the last 2 weeks compared with the control specimens. Figure 16 shows a typical failed MDCB specimen, which depicts pure interfacial fracture. To show interfacial fracture in the initial crack growth of this specimen, the specimen was separated using a wedge. Hence, the later part of the crack propagation was not interfacial and the reader should not be misled by this.

The polyurethane used in this study absorbs some water and water absorption during pressure-cycling might have significantly influenced its mechanical properties and, thus, the adhesive bond strength. Since pressure-cycling is expensive, the extent of water absorption in polyurethane was explored by submerging samples in water at room temperature. Two types of specimens were made: aluminum-sandwiched polyurethane slabs similar to MDCB specimens (for water

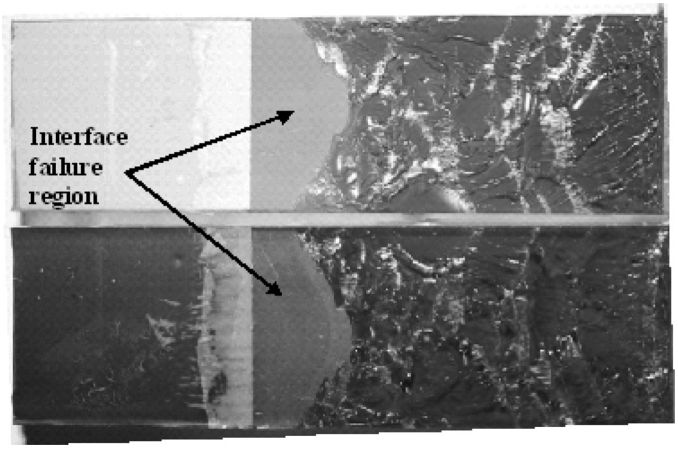

FIGURE 16 Fractured MDCB specimen shows pure interfacial fracture.

absorption testing) and dog bones as per ASTM D412 Standard [19] (for failure load measurements). Figure 17 shows the extent of water absorption for water-soaked polyurethane samples. The mass of absorbed water increased by 100% from the first week of exposure to the fourth week of exposure. Dog bone samples of polyurethane were made and the effect of water absorption on failure load was studied. Figure 18(a) shows typical load-extension diagrams of water-soaked

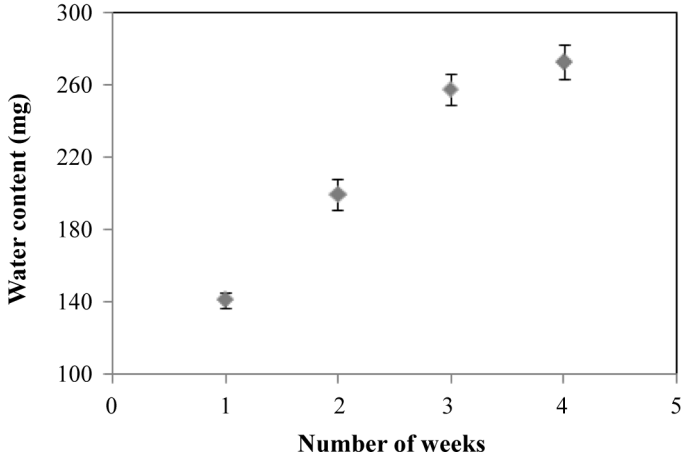

FIGURE 17 Amount of water absorption in polyurethane for water-soaked samples.

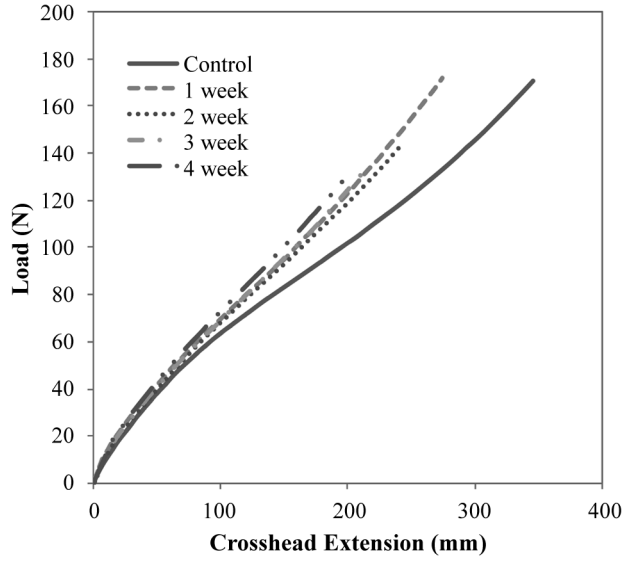

(a)

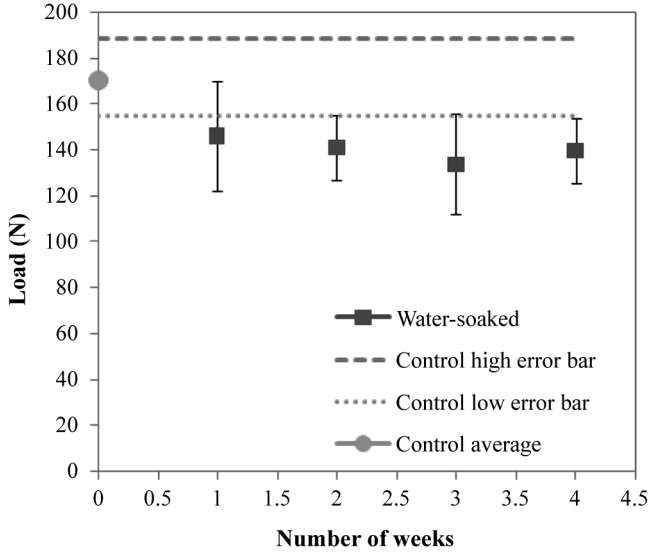

(b)

FIGURE 18 (a) Representative load *vs.* deflection diagrams for water-soaked dog bone samples. (b) Failure load of water-soaked dog bone samples as a function of number of weeks.

dog bone samples. Water-soaking had a significant effect on the failure load of the water-soaked dog bone samples as shown in Fig. 18(b). The failure load for a control sample with no water-soaking is shown as the zero week data point and, again, the horizontal lines are upper and lower error bar lines for the control sample. The water-soaked samples show a significant decrease in failure load values upon increased exposure to water.

Based on the data in Figs. 17 and 18, it can be concluded that the amount of water absorption and its influence on failure load for polyurethane would be much more severe for pressure-cycled samples. Under pressure-cycling, the extent of water penetration is larger and this further reduces the elastic properties compared with water-soaked samples. The water penetration would definitely influence the primer/polyurethane interface and, hence, reduce the adhesive bond strength.

5. CONCLUSIONS

In this experimental investigation of polyurethane/aluminum adhesive bond fracture energy, it was shown that 90° peel tests do not provide clean interfacial fractures without polyurethane cracking. Since polyurethane is a flexible elastomer, the use of a special specimen configuration, namely modified double cantilever beam (MDCB), is essential. Using the MCDB specimen configuration, three types of sample conditioning were utilized: pressure-cycling, water-soaking, and control (no pressure-cycling and no water-soaking). Fracture energy (G_C) was determined as a function of time for both pressure-cycled and water-soaked samples. Comparison of G_C values of the above tests with those of control specimens revealed that pressure-cycling increased G_C initially after 1 week of exposure and then reduced G_C upon further exposure. However, water-soaked samples showed only a slight decrease in G_C values in the third and fourth weeks of pressure-cycling. It is presumed that the reduction in G_C values of the pressure-cycled specimens is caused by water absorption of the polyurethane and its reduction of the failure load of the polyurethane. It is concluded from this study that prolonged pressure-cycling would be problematic to polyurethane/aluminum adhesive bonds of hardware installed outboard of submarine pressure hulls.

ACKNOWLEDGMENTS

The authors would like to acknowledge the partial support of National Science Foundation grant EEC-0332597 and Professor Farhad Azadivar for allocating funds for this project through this grant.

REFERENCES

[1] Shah, Q. H., Hommah, H., Liyas, M. H., and Ismail, A. F., *J. Appl. Sci.* **3**, 476–481 (2005).
[2] Kim, A. S., Besson, J., and Pineau, A., *J. Solids. Struct.* **36**, 1845–1864 (1999).
[3] McCormack, B. A. O., Prendergast, P. J., and O'Dwyer, B., *J. Fat. Fract. Engng. Mater. Struct.* **22**, 33–40 (1999).
[4] Lund, P. G., Evans, A. G., and McMeeking, R. M., *J. Appl. Mech. (Trans ASME).* **56**, 77–82 (1989).
[5] Sugimara, Y., Lim, P. G., Shih, C. F., and Suresh, S., *Acta. Metall. Mater.* **43**, 1157–1169 (1995).
[6] Venables, J. D., *J. Mater. Sci.* **19**, 2431–2453 (1984).
[7] Nitsché, F., *J. Adhes. Sci. Technol.* **4**, 41–55 (1990).
[8] Dauskardt, R. H., Kook, S.-Y., Kirtikar, A., and Ohashi, K. L., *Proceedings of TMS Fall Symposium*. (1997), pp. 479–498.
[9] Bistac, S., Guillemenet, J., and Schultz, J., *J. Adhes.* **78**, 987–996 (2002).
[10] Deb, A., Malvade, I., Biswas, P., and Schroeder, J., *Int. J. Adhes. Adhes.* **28**, 1–15 (2007).
[11] Shatil, G., Saimoto, A., and Ren, X. J., *Engng. Fra. Mech.* **75**, 674–681 (2008).
[12] Toivola, Y., Somerday, B. P., Shediac, R., and Cook, R.F., *J. Mater Res.* **19**, 557–567 (2004).
[13] ASTM D6862-04, Standard Test Method for 90 Degree Peel Resistance of Adhesives, (Am. Soc. Testing & Materials, Philadelphia, 2004).
[14] Kawashita, L. F., Moore, D. R., and Williams, J. G., *J. Adhesion* **80**, 147–167 (2004).
[15] Kawashita, L. F., Kinloch, A. J., Moore, D. R., and Williams, J. G., *Engg. Fract. Mech.* **73**, 2304–2323 (2006).
[16] Othmer, K., *Encyclopedia of Chemical Technology*, 4th Ed., (Wiley-Interscience, Hoboken, 2001), pp. 920–921.
[17] Cantwell, W. J., Scudamore, R., Ratcliffe, J., and Davies, P., *Comp. Sci. Tech.* **59**, 2079–2085 (1999).
[18] Kirtisaevee, H. and Cantwell, W. J., *Poly. Comp.* **25**, 499–509 (2004).
[19] ASTM D412-06, Standard Test Methods for Vulcanized Rubber and Thermoplastic Elastomers—Tension, (Am. Soc. Testing & Materials, Philadelphia, 2006).